Food Biophysics
https://doi.org/10.1007/s11483-024-09867-1

RESEARCH

Comprehensive Analysis of Adsorption–Desorption Isotherms, Drying Kinetics, and Nutritional Quality of Black Soldier Fly (*Hermetia illucens*) Larvae

Manal Lehmad[1] · Youssef EL Hachimi[1] · Patrick Lhomme[2] · Safa Mghazli[1] · Naji Abdenouri[3]

Received: 26 March 2024 / Accepted: 19 July 2024

Abstract
Black soldier fly larvae (BSFL) are gaining attention as an alternative protein source in food and feed, promoting a circular economy, particularly in their dried form. In the literature, monitoring the behavior of larvae in a humid environment has not been established under different conditions of temperature and relative humidity as well as the quality of dried larvae is not always correlated to the conditions of drying. Therefore, this study comprehensively analyses the adsorption–desorption isotherms, drying kinetics, and subsequent quality changes of dried BSFL. Sorption isotherms were assessed at 40, 50, 60, and 70 °C using the gravimetric method, followed by mathematical modelling and determination of thermodynamic variables. Thin-layer drying kinetics were studied in a forced-air oven at the same temperatures, with a subsequent proximate analysis of the dried larvae. Among eight sorption isotherm models evaluated, the Peleg model provided the best fit, revealing type II sorption isotherms with an optimal storage water activity of 0.38. The Page model accurately described the drying kinetics of BSFL across all temperatures. Moisture diffusion coefficients ranged from 6.15×10^{-11} to 2.63×10^{-10} m^2/s, with an activation energy of 48.66 kJ/mol. The dried larvae displayed impressive protein levels, varying from $39.67\pm0.28\%$ to $45.29\pm0.07\%$, exceeding the minimum requirements set in the global insect production industry. Higher drying temperatures significantly impacted the proximate composition, reducing larvae quality. These findings underscore the potential of BSFL as a valuable protein source and enhance the understanding of their sorption behavior and quality attributes during drying. This study contributes to the optimization of drying conditions for improving the quality of BSFL as a sustainable protein alternative.

Keywords Edible insects · Sorption isotherms · Dehydration kinetic · Food and feed

Introduction

Insect farming holds great potential to tackle food security and livelihood challenges by creating jobs, generating income, and minimizing greenhouse gas emissions through a circular economy [1, 2]. Insects serve as a substitute for traditional animal protein sources [3], offering a sustainable and efficient solution to meet the growing global demand for protein. Research on edible insects has significantly evolved over the years, reflecting diverse interests and advancements in fields such as food technology, entomology, and nutritional dietetics [4]. Among the various edible insects, *Hermetia illucens*, commonly known as the Black Soldier Fly (BSF), stands out as a particularly promising candidate in the rapidly expanding insect-farming industry [5].

Black Soldier Fly Larvae (BSFL) possess several advantages. They are highly polyphagous, voracious and efficient converting diverse organic waste into protein and lipid-rich biomass [6, 7]. They can be used to produce various valuable products such as proteins for food and animal feed, fats for biodiesel production, compost for agriculture, and chitin for nutraceutical applications [8, 9].

✉ Manal Lehmad
manal.lehmad@ced.uca.ma

✉ Naji Abdenouri
n.abdenouri@uca.ac.ma

[1] Laboratory of Bioresources and Food Safety, Faculty of Sciences and Techniques, Cadi Ayyad University, 40000 Marrakech, Morocco

[2] Laboratory of Zoology, Research Institute for Bioscience, Mons University, 7000 Mons, Belgium

[3] Laboratory of Control and Computing for Intelligent Systems and Green Energy, Faculty of Sciences and Techniques, Cadi Ayyad University, 40000 Marrakech, Morocco

Published online: 31 July 2024

It is essential to understand the sorption isotherms of BSFL to optimize their drying process and storage conditions. Sorption isotherms, defined under constant pressure and temperature, link equilibrium moisture content with water activity [10]. The isotherm curve can be generated using two approaches. First, by establishing an adsorption isotherm through exposing a dry material to increasing humidity and measuring the weight gain. Second, by obtaining a desorption isotherm by subjecting a wet material to the same humidity levels and measuring the weight loss [11]. Weightings are carried out after reaching the hygroscopic equilibrium between the product and the ambient air. This equilibrium is established by the diffusion of water from the inside of the product towards its periphery, then by diffusion in the drying air. These isotherms are essential for equipment design and optimization, drying process modelling, critical moisture level determination, estimation of thermodynamic properties of adsorbed water in the product, shelf life prediction, and selection of suitable packaging materials [12]. Moreover, they aid in anticipating stability and quality variations during the packaging and storage of dried food products.

While BSFL can be given to animals as fresh feed, it is not feasible on a large scale due to the need for storage, packaging, and transport. Therefore, a suitable preservation method is necessary. The preservation of biological materials such as insects products can be accomplished through the modification of various factors, including temperature, pH, and water activity [13]. Convective drying is widely embraced as a food preservation method due to its effectiveness in reducing water activity. It offers several benefits, including the reduction of weight and volume of foods, extension of shelf life, and simplification of storage, packaging, and transportation. Given these advantages, drying emerges as the most cost-effective method of food preservation [14]. At large-scale insect drying, where enhancing efficiency, conserving energy, and promoting sustainability are critical imperatives, a comprehensive grasp of BSFL drying kinetics plays a central role [15]. This understanding serves as a cornerstone for industrial experts, allowing them to optimize drying parameters, select optimized conditions within the dryer, and minimize energy consumption.

As far as we know, research on processed edible insects has primarily focused on adsorption, as documented by Azzollini et al. [16] for the yellow mealworm (*Tenebrio molitor*) and by Kamau et al. [17] for the house cricket (*Acheta domesticus* L.), the black soldier fly larvae (*Hermetia illucens* L.), and the lesser mealworm (*Alphitobius diaperinus*). In addition, there is a notable lack in the bibliography of models for generating sorption isotherms and the associated thermodynamic properties of moisture exchanges between BSFL and air in a precise and reliable manner. This data is often sought by manufacturers in the field. Furthermore, regarding BSFL drying, the effect of drying technologies has been studied mainly from a nutritional perspective, including BSFL hybrid solar-electric drying [18], freeze-drying [19], microwave drying, and conventional drying [20]. However, there is a gap in the study of the drying phenomenon from a physical perspective to comprehensively characterize and understand the hygroscopic behavior of BSFL.

This study contributes to filling significant gaps in the existing literature on BSFL in two key areas. Firstly, it addresses the mathematical modelling of adsorption and desorption isotherms and the determination of thermodynamic variables describing their sorption isotherms. This exploration aims to validate physical concepts within the models and provide insights into the hygroscopic behavior of the larvae. Secondly, it provides a comprehensive examination of BSFL thin-layer drying kinetics, providing valuable insights into the optimal drying conditions to achieve a well-defined quality tailored to the intended use. Therefore, the objectives of this study were:

- Determine moisture adsorption and desorption isotherms at four different temperatures (40, 50, 60 and 70°C),
- Fit different models to the experimental data of isotherms (adsorption and desorption) and determine the thermodynamic variables,
- Perform convective drying of larvae at four different temperatures (40, 50, 60 and 70°C), adjust different empirical mathematical models to experimental data on drying kinetics and calculate effective diffusivity and activation energy, and
- Determine the effects of convective drying at different temperatures on the nutritional and physicochemical properties of BSFL.

Materials and Methods

This section provides a detailed description of the methodology followed for the analysis of adsorption–desorption isotherms, drying kinetics, and nutritional quality of BSFL. The larvae used in this study were obtained from the startup "EntomoNutris". To standardize the experiments, BSFL were exclusively fed chicken feed, were 13 days old, and underwent a freezing process at -20 °C for 24 h to ensure their euthanasia. We adhered to the guidelines of the International Platform of Insects for Food and Feed (IPIFF) for insect welfare in breeding and harvesting the larvae [21]. The experimental methodology is illustrated and clarified with a schematic diagram presented in Fig. 1. Three

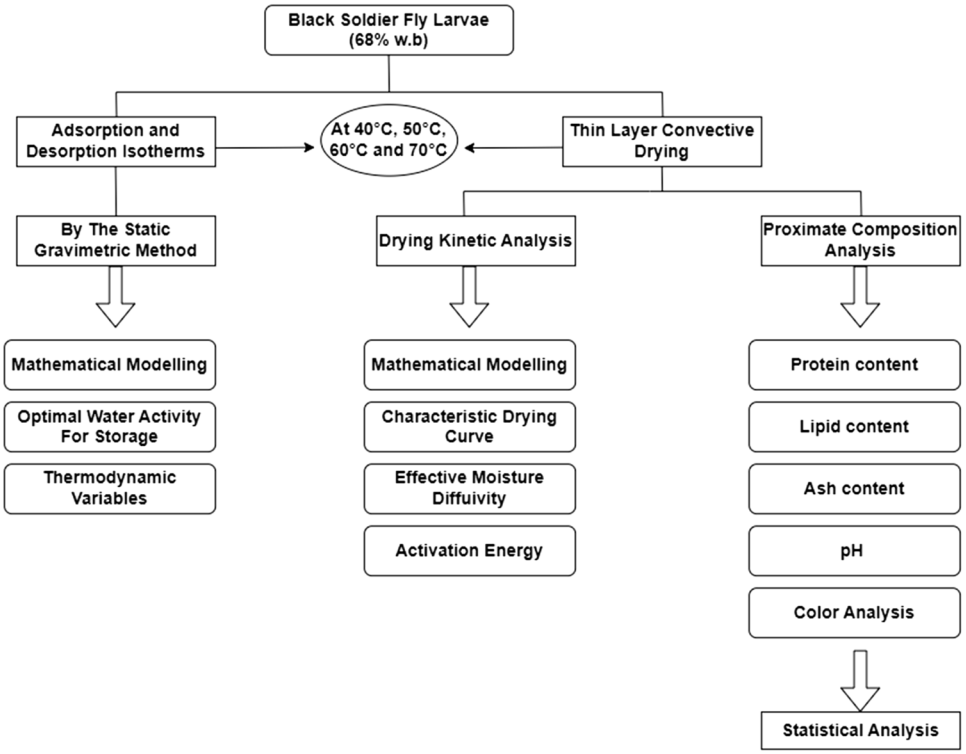

Fig. 1 Schematic diagram of the experimental methodology

replicates were conducted throughout the entire study to evaluate variability.

Sorption Isotherm Experiments

After thawing, the larvae were divided into two groups. The first group was used immediately for desorption isotherm analysis. The second group, designated for adsorption isotherm analysis, was dried in a forced convection oven at 60 °C until reaching a stable weight. Both adsorption and desorption isotherms were examined at four distinct temperatures: 40, 50, 60, and 70 °C. The static gravimetric method was employed for this analysis, utilizing six different saturated salt solutions (KOH, $MgCl_2$, K_2NO_3, $NaNO_3$, KCl, and $BaCl_2{\cdot}2H_2O$), as described by [22, 23]. These solutions were used to maintain relative humidity levels ranging from 5 to 90% (as outlined in Table 1).

Mathematical Modelling of Sorption Isotherms

The moisture sorption data obtained from the experiments were analyzed using eight mathematical models (Table 2) through nonlinear regression: Enderby, Peleg, Oswin, Modified Oswin, Modified Henderson, Smith, Halsey, and GAB models. The selection of the most suitable model was determined following the procedures outlined in the statistical analysis section. For a given water activity, the equilibrium moisture content X_{eq} of each sample is determined as follows:

$$X_{eq} = \frac{m_h - m_S}{m_S} \tag{1}$$

where X_{eq} is the equilibrium moisture content (kg water/kg dry matter), m_h is the sample weight at equilibrium (kg) and ms is the dry weight of the sample (kg). m_s was

Table 1 Standard values of the water activities of the salts used in the experiments [24]

Temperature	KOH	$MgCl_2$	K_2CO_3	$NaNO_3$	KCl	$BaCl_2.2H_2O$
40 °C	0.0626	0.3159	0.4230	0.7100	0.8232	0.8910
50 °C	0.0572	0.3054	0.4091	0.6904	0.8120	0.8823
60 °C	0.0550	0.2930	0.3952	0.6708	0.8030	0.8736
70 °C	0.0530	0.2780	0.3813	0.6512	0.7950	0.8649

Table 2 Mathematical models applied to black soldier fly larvae's sorption curves

Model name	Equation	References	Equation No
Enderby	$Xeq = \left[\frac{A}{1-Ba_w} + \frac{C}{1-Da_w}\right]a_w$	[25]	(2)
Peleg	$Xeq = A(a_w)^C + B(a_w)^D$	[26]	(3)
Oswin	$Xeq = \mathrm{A}\left(\frac{a_w}{1-a_w}\right)^B$	[27]	(4)
Modified Oswin	$Xeq = (\mathrm{A} - \mathrm{BT})\left(\frac{a_w}{1-a_w}\right)^C$	[27]	(5)
Modified Henderson	$Xeq = \left(\frac{\ln(1-a_w)}{-\mathrm{A(T+B)}}\right)^{1/C}$	[28]	(6)
Smith	$Xeq = A - Bln(1 - a_w)$	[29]	(7)
Halsey	$Xeq = \left(\frac{-\mathrm{A}}{\ln(a_w)}\right)^{1/B}$	[30]	(8)
GAB (Guggenheim–Anderson–De Boer)	$Xeq = \frac{\mathrm{ABC}a_w}{(1-\mathrm{B}a_w)(1-\mathrm{B}a_w+\mathrm{BC}a_w)}$	[31]	(9)

Note: In the table, X_{eq} represents equilibrium moisture, a_w denotes water activity, T stands for temperature, and A, B, C, and D are the model's parameters

determined through oven drying at a temperature of 105 °C until a constant mass is achieved.

Determination of the Optimal Water Activity for Storing Black Soldier Fly Larvae

The analysis of adsorption and desorption isotherms allows for the determination of the optimal water activity for BSFL preservation, as well as the associated equilibrium water content at the end of the drying process. To determine the optimal water activity, a polynomial decomposition of the equilibrium water content (X_{eq}) as a function of water activity is performed. This approach enables the calculation of the water activity value at which the second derivative of X_{eq} reaches zero (inflection point), thereby identifying the optimal water activity for storage.

Determination of the Thermodynamic Properties of Black Soldier Fly Larvae

Isosteric Heat of Sorption and Differential Entropy

The net isosteric heat of sorption (q_{st}), also known as differential enthalpy, quantifies the energy involved in the binding of water to the product. The calculation of q_{st} is achieved using a relationship derived from the Clausius–Clapeyron equation (Eq. (10)). The differential sorption entropy (ΔS) evaluates the level of microscopic disorder within the system and is determined from the intercept of the Clausius-Clapeyron plot (Eq. (10)).

$$\ln\left(a_w\right) = \frac{-q_{st}}{\mathrm{R}}\left(\frac{1}{T}\right) + \frac{\Delta S}{R} \tag{10}$$

where a_w is the water activity, qst is the net isosteric heat of sorption (J/mol), T is the absolute temperature (K), R is the universal gas constant (8.314 kJ/(mol.K)) and ΔS the differential entropy (J/(mol.K)).

Compensation Theory

The enthalpy-entropy compensation theory, also known as the isokinetic theory, posits that there is a linear relationship between the differential enthalpy (qst) and the differential entropy (ΔS). This relationship,derived from the Gibbs–Helmholtz equation, can be expressed as follows:

$$q_{st} = T_\beta \Delta S + \Delta G_\beta \tag{11}$$

where T_β represents the isokinetic temperature, at which all reactions in a series occur simultaneously under isokinetic conditions, and ΔG_β denotes Gibbs free energy. This parameter measures the spontaneity of the sorption process; it is considered non-spontaneous when ΔG_β is positive and spontaneous when ΔG_β is negative.

The validity and accuracy of the compensation theory can be demonstrated by comparing the isokinetic temperature (T_β) with the theoretically determined harmonic mean temperature (T_{hm}) as described in Eq. (12). According to [32, 33], the compensation theory holds true only when T_β deviates from T_{hm}. Specifically, when $T_\beta > T_{hm}$, enthalpy drives the sorption process, while $T_\beta < T_{hm}$ suggests entropy as the driving force.

$$T_{hm} = \frac{n}{\sum_1^N 1/T} \tag{12}$$

where n is the number of isotherms.

Drying Kinetics Experiments

After the larvae underwent a thawing process at room temperature for 5 h (~25 °C), 500 g of the larvae were evenly spread in a thin layer within a forced-air oven (AX 30, Carbolite Gero, Germany). The dimensions of the experimental dryer are 0.295 m×0.30 m×0.32 m, and the bed density of the BSFL distributed on the two racks of the dryer is approximately 2.60 kg/m^2. Drying experiments were then conducted at four distinct temperatures: 40, 50, 60, and 70 °C, with a drying air velocity of 5.8 m/s. To monitor the dynamics of larvae mass change during the drying process, three samples of 10 g each were periodically taken from the initial 500 g of larvae placed on the shelf. These samples were weighed at 10-min intervals during the first four hours of drying, and subsequently every hour until reaching a constant weight, in order to determine the moisture content (X_t) (Eq. (13)).

$$X_t = \frac{m_t - m_d}{m_d} \tag{13}$$

In this context, X_t (in kg water/kg dry matter) and m_t (in kg) signify the changes in moisture content and mass of the larvae over the drying time (t) respectively, and m_d (in kg) represents the measured dried mass of the product.

Mathematical Modelling of Drying Curves

The experimental moisture ratio changes over time were fitted to ten different models (Table 3) using nonlinear regression. These models include the Newton, Page, Modified Page, Henderson and Pabis, Logarithmic, Two-term, Wang and Singh, Two-term exponential, Diffusion approximation, and Midilli-Kucuk models. The assessment of the most suitable model was conducted following the procedures outlined in the statistical analysis section. To ascertain the initial moisture content of BSFL, the oven method was employed, subjecting the samples to 105 °C until a constant mass is achieved. The obtained initial moisture content (X_0) was 2.13 (d.b) or 68% (w.b). The moisture ratio (MR) and the drying rate (DR) of BSFL obtained during drying at different temperatures were calculated using Eqs. (14) and (15), according to Da Silva et al. [34]:

$$MR = \frac{X_t - X_{eq}}{X_0 - X_{eq}} \tag{14}$$

$$DR = \frac{-dX}{dt} = (X_0 - X_{eq})\left[\frac{-dMR}{dt}\right] \tag{15}$$

where X_0, X_t and X_{eq} are moisture contents at instant t_0, t and equilibrium (kg water/kg dry matter, d.b). X_{eq} was determined by monitoring the drying kinetics until a constant weight was achieved, indicating an equilibrium state. At this point, X_{eq} was calculated using Eq. (1).

The Characteristic Drying Curve (CDC)

The application of Van Meel's theory [45] enables the investigation of how drying temperature affects the drying kinetics of BSFL by employing a characteristic drying curve (CDC). This curve is constructed by maintaining constant drying temperature, air velocity, and relative humidity, resulting in a uniform drying rate curve. Utilizing this CDC allows for the extrapolation of data regarding the drying kinetics of BSFL in a generalized manner. The CDC equation is defined by f=f (MR) as shown in Eq. (26):

$$f = \frac{\left(\frac{-dX}{dt}\right)_t}{\left(\frac{-dX}{dt}\right)_{t=0}} \tag{26}$$

Under constant experimental conditions, including temperature, humidity, velocity, and size of the BSFL, the

Table 3 Mathematical models applied to black soldier fly larvae's drying curves

Model name	Equation	References	Equation No
Newton	$MR = \exp(-kt)$	[35]	(16)
Page	$MR = \exp(-kt^n)$	[36]	(17)
Modified Page	$MR = \exp(-kt)^n$	[37]	(18)
Henderson and Pabis	$MR = a.\exp(-kt)$	[38]	(19)
Logarithmic	$MR = a.\exp(-kt) + c$	[39]	(20)
Two-term	$MR = a.\exp(-k_0 t) + b.\exp(-k_1 t)$	[40]	(21)
Two-term exponential	$MR = a.\exp(-kt) + (1-a).\exp(-kat)$	[41]	(22)
Wang and Singh	$MR = 1 + a.t + bt^2$	[42]	(23)
Diffusion approximation	$MR = a.\exp(-kt) + (1-a)\exp(-kbt)$	[43]	(24)
Midilli-Kucuk	$MR = a.\exp(-kt^n) + bt$	[44]	(25)

characteristic drying curve should confirm the properties outlined in Eq. (27):

$$\begin{cases} f = 0 \; for \; MR = 0 \\ 0 \le f \le 1 \; for \; 0 \le MR \le 1 \end{cases} \tag{27}$$

Determination of Effective Moisture Diffusivity and Activation Energy

The term "effective moisture diffusivity" (D_{eff}) (m^2/s) encompasses various mechanisms responsible for the transportation of water within a sample. It is the key physical feature that allows modelling of the mechanism of moisture transport from the core to the surface during BSFL drying. The BSFL were considered as infinite cylinders, given that the length of the larvae is much greater than their diameter. This article assumes that the liquid diffusion model is appropriate for describing thin-layer water transport. It employs a third-kind or convective boundary condition, where the internal diffusive mass flow at the larvae's boundary is assumed to equal the external convective flow near this boundary [46].The analytical solution of Fick's second law for this geometric shape was utilized to estimate the diffusion coefficient of BSFL at various drying temperatures [47].

The diffusion equation expressed in cylindrical configuration is as bellow:

$$\frac{\partial X}{\partial t} = \frac{1}{r}\frac{\partial}{\partial t}\left(rD_{eff}\frac{\partial X}{\partial r}\right) \tag{28}$$

This equation can be analytically resolved by considering the following hypotheses [34]:

- At the initial state, the moisture distribution is considered uniform;
- The material is considered isotropic and homogeneous;
- The geometric shape of the medium remains the same throughout the diffusion operation;
- Inside matter, the diffusion of water occurs only by diffusion;
- The effective diffusivity does not vary during diffusion;
- The convective mass transfer coefficient is constant during diffusion.

By considering of the third kind, the boundary condition is expressed by the convection–diffusion equation at each time t (at r = R):

$$-D_{eff}\left.\frac{\partial X(r,t)}{\partial r}\right|_{r=R} = h\left(X(r,t)|_{r=R} - X_{eq}\right) \tag{29}$$

where,

- h is the convective mass transfer coefficient,
- X(r,t) is the moisture content at radial distance r and time t,
- X_{eq} is the equilibrium moisture content in a solid of given drying matter,
- R is the radius of the infinite cylinder,
- r is the variable radial position in the cylinder.

The solution X(r,t) of Eq. (28) with the boundary condition Eq. (29) can be obtained by separation of variables [48, 49], and the average moisture content $\overline{X}(t)$ can be computed by using the next equation:

$$\overline{X}(t) = \frac{1}{V}\int X(r,t)dV \tag{30}$$

where V is the volume of the cylinder.

The expression of average moisture content $\overline{X}(t)$ is given as follows [50]:

$$\overline{X}(t) = X_{eq} - (X_{eq} - X_0)\sum_{n=1}^{\infty} B_n \exp(-\mu_n^2 \frac{D_{eff}}{R^2}t) \tag{31}$$

$$B_n = \frac{4B_i^2}{\mu_n^2(B_i^2 + \mu_n^2)} \tag{32}$$

$$J_0(\mu_n)B_i - \mu_n J_1(\mu_n) = 0 \tag{33}$$

In this context, R is the radius of the infinite cylinder, D_{eff} is the effective diffusivity, μ_n are the roots of the transcendental equation (Eq. (33)), B_i is the mass transfer Biot number, J_0 and J_1 are the Bessel functions of the first kind with order 0 and 1, respectively.

In this work, we have employed the optimization algorithm "Convective Adsorption–Desorption" software version 3.2 (Federal University of Campina Grande, PB, Brazil) [51], introduced by Da Silva et al. [50] to calculate the effective mass diffusivity D_{eff} and determine the graphs of the diffusive model fitted to our experimental data. Additionally, to minimize truncation errors, the selection of the number of terms in the series given in Eq. (31) representing the solution of the diffusion equation was determined according to findings from prior studies conducted by Da Silva et al. [47, 50, 52].

The activation energy (E_a) measures how easily water molecules can surpass an energy barrier when they are transported through the product's pathways. The diffusion coefficient obeys the Arrhenius law, as shown in Eq. (34):

$$D_{eff} = D_0 \; exp\left[-\frac{E_a}{RT_{abs}}\right] \tag{34}$$

where E_a is the activation energy (kJ/mol), D_0 is the pre-exponential factor of the Arrhenius equation (m^2/s), R is

the universal gas constant (8.314 J/ mol.K) and T_{abs} is the absolute temperature of drying BSFL (K).

Characterization of Black Soldier Fly Larvae

Proximate and physicochemical analyses were conducted on fresh thawed larvae and dried larvae at four temperatures (40 °C, 50 °C, 60 °C and 70 °C) using a forced-air oven dryer (AX 30, Carbolite Gero, Germany). The dry matter content was assessed using the AOAC 950.46 method, which involves oven drying samples at a temperature of 105 ± 3 °C until constant weight. The ash content was determined using the official method 942.05. Lipids were extracted using the Soxhlet extraction method, following the procedure AOAC 920.39. Protein content was determined using the Kjeldahl protocol according to the AOAC 984.13 method, with a nitrogen-to-protein conversion factor of 4.76 [53]. The color of fresh and dried larvae was assessed using a Minolta Chroma meter CR-400 (Minolta Co., Osaka, Japan) that was calibrated with a standard white plate. Measurements were taken using illuminant D65 and a 10° standard observer. The color values were recorded in terms of L*, a*, and b* coordinates. For pH measurement, 1 g of BSFL meal was homogenized for 30 s in 9 mL of distilled water. Each analysis was conducted in triplicate.

Statistical Analysis

The parameters of the sorption models and the kinetic parameters of the drying equations were estimated by fitting mathematical models to the experimental data using the direct nonlinear regression method with the Levenberg–Marquardt procedure in OriginPro 2022 software. Various statistical criteria were employed to assess the goodness of fit for each model, including the coefficient of determination (r^2), reduced chi-square (χ^2), and root mean square errors ($RMSE$). A lower $RMSE$ *and* χ^2, along with a higher r^2, indicate a higher quality of fit for the model (Eqs. (35–37)). One-way analysis of variance (ANOVA) was used to examine the variances in mean values of proximate composition and physicochemical properties. Tukey's post hoc test was used for means comparisons, with significance determined at a P-value of less than 0.05. The analysis was performed using IBM SPSS statistics 25 software.

$$RMSE = \frac{\sum_{i=1}^{n}(MR_{pre,i} - MR_{exp,i})}{N} \tag{35}$$

$$\chi^2 = \frac{\sum_{i=1}^{n}(MR_{exp,i} - MR_{pre,i})^2}{N - L} \tag{36}$$

$$r^2 = \frac{\sum_{i=1}^{n}(MR_i - MR_{pre,i}).\sum_{i=1}^{n}(MR_i - MR_{exp,i})}{\sqrt{\left[\sum_{i=1}^{n}(MR_i - MR_{pre,i})^2\right]\left[\sum_{i=1}^{n}(MR_i - MR_{exp,i})^2\right]}} \tag{37}$$

where $MR_{pre,i}$ and $MR_{exp,i}$ are predicted and experimental moisture ratio. N is the number of observations and L is the number of constants.

Results and Discussion

Sorption Isotherms

The hygroscopic equilibrium of BSFL was reached after 26 days for desorption and after 19 days for adsorption. Given that BSFL are exposed to a variety of temperatures during storage and processing, and that temperature changes affect water activity, the effect of temperature on the sorption isotherm becomes critical. Temperature also affects the mobility of water molecules and the dynamic equilibrium between the adsorbed and vapor phases [11]. Therefore, to demonstrate the impact of temperature, Fig. 2 shows the BSFL's adsorption and desorption isotherms for each of the four temperatures investigated separately.

According to Fig. 2, when the temperature decreases at a constant water activity, the equilibrium moisture content (X_{eq}) of the larvae increases. This is due to a decrease in the larva's hygroscopicity, making it less able to retain moisture [54]. This phenomenon can be elucidated by considering that elevated temperatures induce greater molecular mobility and heightened energy levels within water molecules. This augmented molecular activity weakens the intermolecular forces governing water molecules, causing their detachment from sorption sites and thereby leading to a decrease in equilibrium water content [55]. Additionally, at lower temperatures, proteins have greater abilities to bind water [56]. In this regard, similar findings for the sorption curves have been documented in the literature [57, 58]. The adsorption and desorption isotherms of BSFL exhibit a type II isotherm, according to Brunauer's classification, which is commonly observed in protein-rich products such as insects [16, 17]. These isotherms display a non-linear and sigmoidal shape, indicating an asymptotic trend as the water activity approaches unity ($a_w = 1$) [59]. The observations in Fig. 2 demonstrate that at low water activity, water molecules are adsorbed onto active binding sites. As the water activity increases, more water molecules form covalent bonds and contribute to the bound water, leading to the formation of a less tightly linked multilayer moisture. At water activities above 0.8, the equilibrium moisture content increases exponentially due to additional multilayer sorption, particularly in higher weight constituents. This

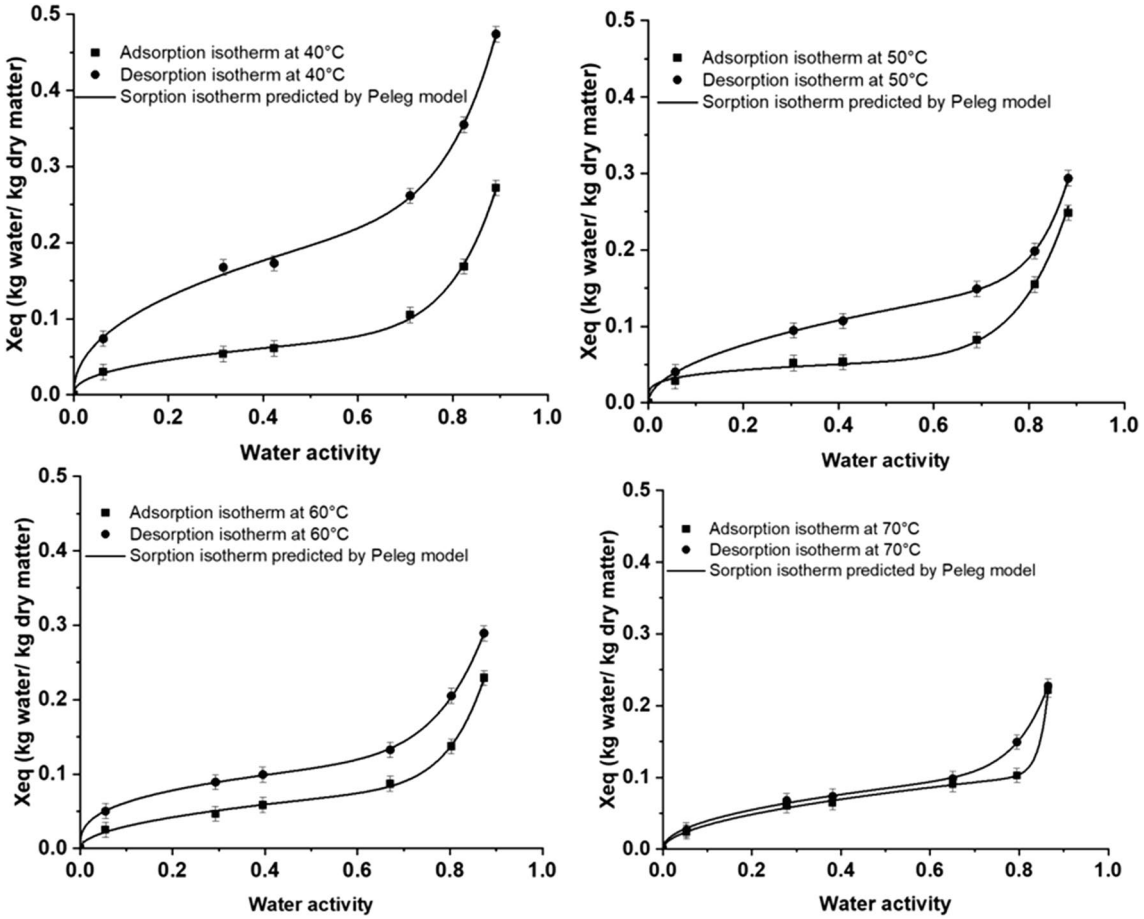

Fig. 2 Sorption isotherm and hysteresis phenomenon of black soldier fly larvae at 40, 50, 60, and 70 °C

phenomenon provides evidence of the progressive thickening of the adsorbed water layer, a characteristic feature of type II isotherms observed in non-porous or macroporous substances [60]. Cricket and mealworm larvae were also reported as exhibiting type II isotherm [16, 17]. The same for other high protein food including lean beef [61] and pirarucu (*Arapaima gigas*) filet [62].

Also according to Fig. 2, hysteresis is observed across the entire range of water activities since at a given temperature, the sorption curves differ. Furthermore, at a constant water activity, the equilibrium moisture content of the desorption isotherm is higher than that of the adsorption isotherm. The presence of hysteresis can be attributed to the irreversible changes that occur in the structure and porosity of the product during drying, particularly the transition from a water activity of 1 to a water activity below 0.6. This phenomenon is linked to the substrate's composition and structure [58]. During adsorption, when the relative humidity of the environment is higher than that inside the pores of the larvae, water is desorbed from the fine capillaries, leading to changes in humidity within the pores. Conversely, during desorption, the initially saturated pores release liquid when the air pressure in the surrounding environment becomes lower than the pressure of the liquid inside the pores [63]. As mentioned by [64], hysteresis can serve as an indicator of food quality, and minimizing or eliminating the hysteresis loop has been linked to improved product stability during storage. In the case of BSFL, it was observed that increasing the temperature led to a significant reduction in both the hysteresis loop and moisture content. This finding suggests an enhanced stability of the product under higher temperatures.

Modelling of Sorption Experimental Data

The measurement and modelling of sorption isotherms of food products have garnered significant attention from researchers due to their relevance in industrial applications. In this work, experimental moisture sorption data of BSFL was collected at temperatures of 40, 50, 60, and 70 °C. Eight different models, namely Enderby, Peleg, Oswin, Modified Oswin, Modified Handerson, Smith, Halsey, and GAB models, were employed to fit the experimental data. The estimated coefficients and the statistical

Table 4 Estimated coefficients for different moisture sorption models to describe the adsorption and desorption isotherms of black soldier fly larvae

Model used	Parameters	40 °C		50 °C		60 °C		70 °C	
		Ads	Des	Ads	Des	Ads	Des	Ads	Des
Enderby	A	1.193	1.952	1.631	0.990	0.018	2.040	0.002	0.014
	B	-25.670	-10.950	-41.081	-8.061	1.045	-23.321	1.139	1.059
	C	0.024	0.045	0.022	0.018	0.823	0.027	0.480	0.780
	D	1.013	0.975	1.026	1.036	-16.381	1.012	-4.461	-9.566
Peleg	A	0.089	0.591	0.546	0.172	0.646	0.505	0.112	0.658
	B	0.538	0.266	0.071	0.694	0.092	0.133	59.631	0.117
	C	0.415	8.558	8.844	0.512	11.217	8.444	0.521	11.865
	D	9.243	0.452	0.308	13.281	0.494	0.334	42.897	0.473
Oswin	A	0.067	0.198	0.059	0.116	0.063	0.115	0.070	0.085
	B	0.646	0.397	0.691	0.426	0.634	0.446	0.544	0.489
Modified Oswin	A	20.533	20.599	25.529	25.558	30.531	30.557	35.531	35.542
	B	0.511	0.510	0.509	0.508	0.507	0.507	0.506	0.506
	C	0.646	0.397	0.691	0.426	0.634	0.446	0.544	0.489
Smith	A	0.004	0.051	0.004	0.027	0.006	0.027	0.013	0.016
	B	0.106	0.185	0.099	0.116	0.094	0.117	0.085	0.095
Halsey	A	0.020	0.026	0.022	0.012	0.019	0.015	0.014	0.013
	B	1.295	1.959	1.217	1.811	1.283	1.730	1.416	1.566
GAB	A	0.024	0.109	0.028	0.061	0.028	0.056	0.028	0.027
	B	1.021	0.857	1.003	0.888	0.999	0.918	1.001	1.015
	C	0.484	1.882	1.879	1.677	0.904	1.566	1.630	0.869

Table 5 Average values of sorption isotherm's modelling parameters

Models	r^2	χ^2	*RMSE*
Enderby	0.9889	0.00007	0.00006
Peleg	0.9994	0.00001	0.00004
Oswin	0.9654	0.0003	0.0015
Modified Oswin	0.9653	0.0004	0.00150
Modified Handerson	0.9338	0.0008	0.00319
Smith	0.9352	0.00065	0.00327
Halsey	0.9784	0.00018	0.00091
GAB	0.9733	0.00121	0.000303

averages of the parameters have been compiled and presented in Table 4 and Table 5, respectively.. The Peleg model, an empirical sorption model with four constants, exhibited the best fit for the adsorption and desorption isotherms of BSFL within the examined temperature range. This model showed the higher r^2 value which was of 0.9994 and the lowest χ^2 and *RMSE* values, which were of 0.00001 and 0.00004, respectively, indicating a good fit, a strong correlation and a minimal deviation from the experimental results. Figure 2 displays a satisfactory alignment and correspondence between the experimental values of equilibrium moisture and the predictions made by Peleg's model.

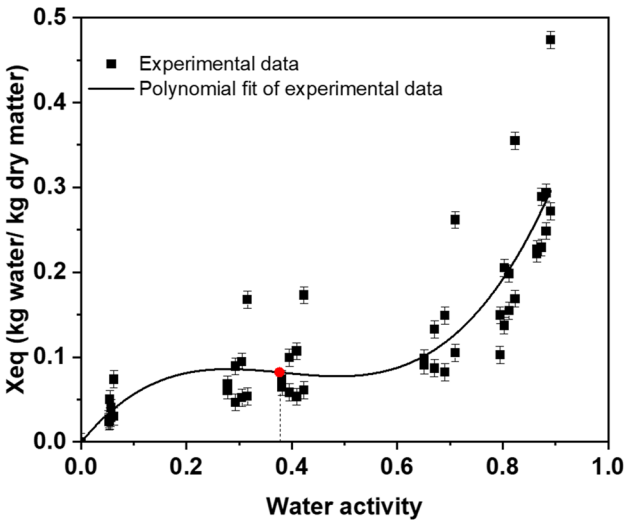

Fig. 3 Determination of optimal water activity for black soldier fly larvae

Optimal Condition for Storage of Black Soldier Fly Larvae

To maintain the stability of BSFL during storage, the analysis of adsorption and desorption isotherms is conducted to identify the optimal water activity level for conservation. Figure 3 depicts the experimental sorption data curves of

BSFL. The sorption isotherm curve is represented by a third-degree polynomial equation, as indicated by Eq. (38):

$$X_{eq} = 1.87(aw)^3 - 2.16(aw)^2 + 0.76(a_w) - 0.0007 \quad (38)$$

The deduced optimal water activity is $a_w = 0.38$. According to the literature, for dry biological products, a water activity of 0.2 to 0.4 is considered optimal for achieving the monolayer state and maximizing product's shelf life. Chemical reactions that require water begin to occur at water activities above this range, while both below and above this range, the rate of lipid oxidation increases [65]. Therefore, the value obtained of the optimal water activity of BSFL is in agreement with the general stability domain of biological products and it is closed to that found for larvae of yellow mealworm (*Tenebrio molitor*) [16].

Determination of the Thermodynamic Properties of Black Soldier Fly Larvae

Isosteric Heat of Sorption and Differential Entropy

The isosteric heat of sorption, also known as the differential enthalpy, provides information about the state of water retained by a solid material. It is important to note that the definition of net isosteric heat varies depending on whether we are discussing adsorption or desorption isotherms. In the case of adsorption, it quantifies the energy released during sorption, which can be challenging to measure due to its small amounts [11]. For desorption, it represents the energy required to attach water to the substrate, indicating the additional heat, beyond the heat of vaporization of pure water, needed to break the bond between the water and the substrate in order to dehydrate it [11]. Figure 4 presents the net isosteric heat of sorption for BSFL within the temperature range of 40 °C to 70 °C. Regarding the desorption isotherm, a high net isosteric heat of sorption ($q_{st} = 62.38$ kJ/mol) was observed at a low equilibrium moisture content ($X_{eq} = 0.03$ kg water/kg d.b), indicating a strong binding energy for water removal. This implies that more energy is required to extract water from the larvae as the drying process progresses. This behavior may be attributed to the BSFL's higher resistance to water movement from the interior to the surface of the product. The differential enthalpy decreases in tandem with increasing equilibrium moisture content, as a higher surface coverage with water results in reduced interaction between the water and the surface [66]. Obviously, the isosteric heat of desorption is higher than that of adsorption (at $X_{eq} = 0.03$ kg water/kg d.b, q_{st} for adsorption equals 8.87 kJ/mol, while it equals 62.38 kJ/mol for desorption). This shows that the energy needed for desorption is higher than that needed for adsorption. When moisture content equilibrium reached 0.2 (kg water/ kg d.b), q_{st} was close to zero, indicating that the total isosteric heat of sorption was similar to the latent heat of vaporization of water. Thus, the presence of water poses the risk of causing severe microbiological, chemical, and biochemical degradation [65]. Similar results were found for cricket meal [17].

The differential entropy quantifies the intensity of the interaction between water molecules and the product, and it is directly linked to the number of available adsorption sites for water molecules at a specific energy level [67]. Figure 5 depicts the change in differential entropy of BSFL in relation to equilibrium moisture content. Notably, the curve exhibits a resemblance to the pattern observed in the net isosteric heat

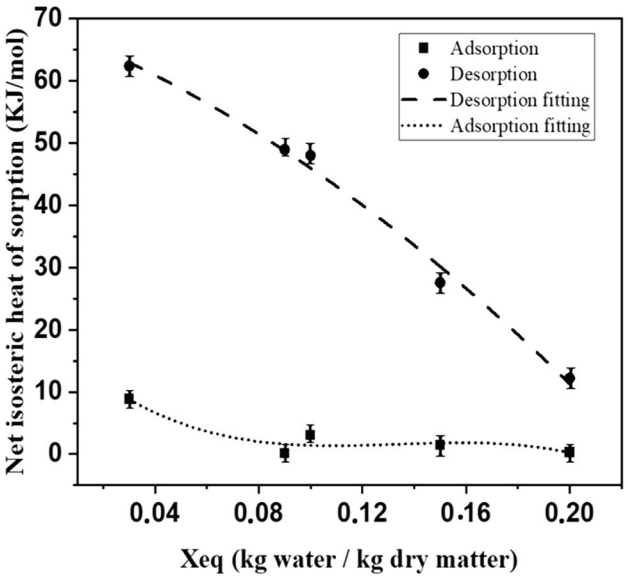

Fig. 4 Net isosteric heat of sorption of black soldier fly larvae as a function of equilibrium moisture content

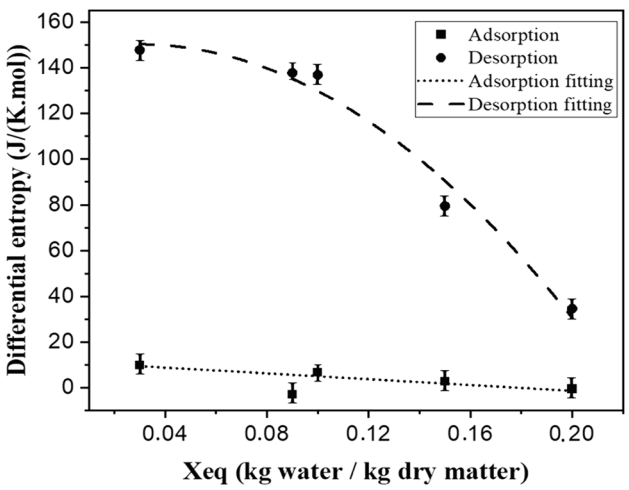

Fig. 5 Differential entropy of black soldier fly larvae as a function of equilibrium moisture content

graph illustrated in Fig. 4. As per the second law of thermodynamics [68], a process is considered reversible if the total entropy changes for all subsystems involved in the process remain constant. However, since the entropy of a system can only increase, it is evident that the sorption of BSFL is an irreversible process. Clearly, the differential entropy of desorption is greater than that of adsorption (at $X_{eq} = 0.03$ kg water/kg d.b, ΔS for adsorption is 9.9221 J/(mol.K), while it is 150.699 J/(mol.K) for desorption). This disparity indicates that desorption requires more energy compared to adsorption due to the increased molecular disorder. This phenomenon occurs during the drying process when bonds are disrupted to remove existing water, leading to an increase in disorder. Consequently, BSFL have a propensity to readily absorb water molecules, while the drying of BSFL becomes challenging at lower water content.

Compensation Theory

The enthalpy-entropy compensation theory states that the rise in enthalpy during the non-covalent interaction between two molecules is often accompanied by a corresponding decline in entropy [69]. This phenomenon is attributed to the isokinetic effect, also known as the compensation effect. Consequently, this theory thermodynamically illustrates the interplay between structuring and destructuring of water. It can be employed to assess the energy required to compensate for the Gibbs energy, which represents the energy needed to maintain the product in equilibrium with its surrounding environment. Figure 6 represents the correlation between net isosteric heat of sorption and differential entropy for BSFL. It indicates a strong linear correlation ($r^2 = 0.9898$ for desorption and $r^2 = 0.9648$ for adsorption) assuming that the compensation theory exist.

As T_β (354.682 K for adsorption and 334.968 K for desorption) was higher than T_{hm} (328.25 K), the sorption process is enthalpy-driven concluding that during the process, the microstructure of the BSFL did not undergo significant changes.

The Gibbs free energy ΔG_β is an essential factor to increase the activity of adsorption sites. The free energy value is positive for adsorption ($\Delta G_\beta = 559.19$ J/mol) while it is negative for desorption ($\Delta G_\beta = -1178.91$ J/mol). It suggests that the adsorption sorption is a forced or non-spontaneous process since it is necessary to give humidity and change the ambient conditions for the product to gain water (requiring a supply of energy to be able to carry out). Whereas the desorption process is spontaneous since the product tends to release water.

Experimental Drying Curves of Black Soldier Fly Larvae

The initial water content of BSFL was 2.13 kg water/kg dry matter, and it was subsequently reduced to a final water content ranging between 0.08 and 0.1 kg water/kg dry matter. Figure 7 illustrates how moisture content evolves with drying time across four different drying temperatures (40, 50, 60, and 70 °C). It is evident that as temperature and drying time increase, moisture content undergoes a significant reduction, exhibiting an exponential decay pattern. Moreover, it's important to highlight that in the drying curve of BSFL, the initial phase (phase 0) and the constant drying rate period (Phase I) are absent, while phase II (the falling drying rate period) is

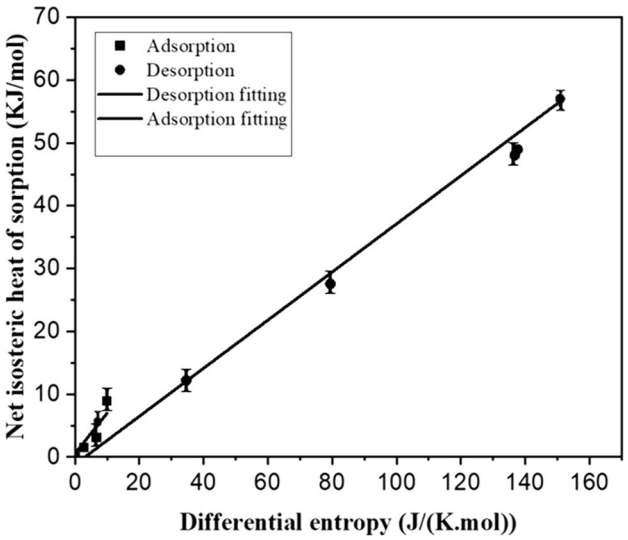

Fig. 6 Compensation theory of black soldier fly larvae

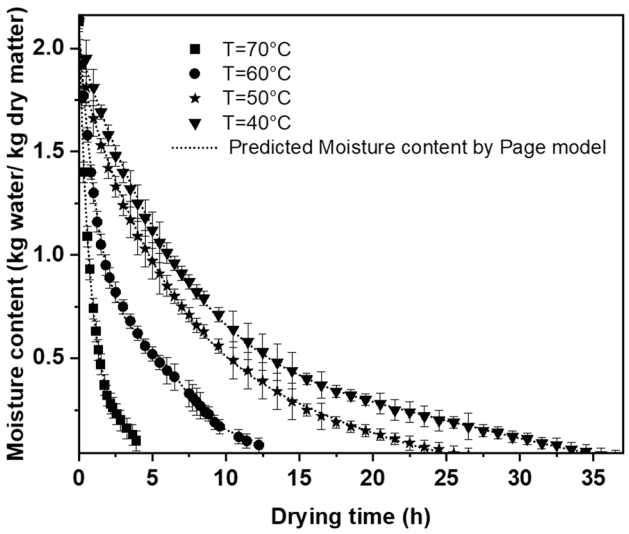

Fig. 7 Evolution of moisture content of black soldier fly larvae as function of drying time at four temperatures

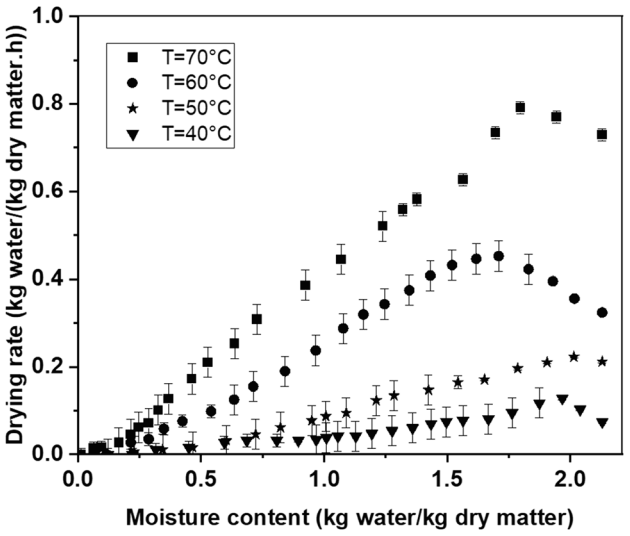

Fig. 8 Variation of drying rate as a function of moisture content at four temperatures

observable. Phase II encompasses two distinct processes: the transfer of moisture from the material's interior to the surface and the subsequent removal of surface moisture. This observation holds true for various other biological products as well (Park and Yoon, 2019; Tanwanichkul, 2023).

Figure 8 illustrates the evolution of drying rate as a function of moisture content at four drying temperatures. The drying rate consistently increases as the drying temperature increases; this is primarily attributed to water evaporation under the influence of temperature. Initially, the drying rate is notably high, owing to the fast evaporation of free water. However, as drying time progresses, the drying rate progressively decreases due to the slower evaporation of bound water, which is a lengthier process. Furthermore, by increasing the temperature, the drying rate of BSFL increases. That is because of the heightened excitement of water molecules at high thermal conditions leading to rapid evaporation. Therefore, the drying kinetics of BSFL is indeed influenced by the drying temperature. Similar trends have been identified for house cricket (*Acheta domestica),* yellow mealworm (*Tenebrio molitor),* and other food products [16, 72, 73].

Mathematical modeling of drying curves

The experimental data were fitted with ten mathematical models to determine a suitable representation of the drying kinetics. Table 6 contains the estimated kinetic parameters for each of the models used to fit the experimental data of moisture ratio, while Table 7 contains the statistical results related to those kinetic parameters.

Table 6 The estimated kinetic parameters of the fitted mathematical models describing the kinetics of black soldier fly larvae

Model used	Kinetic parameters	40 °C	50 °C	60 °C	70 °C
Newton	k	0.1548	0.2756	0.4601	1.8375
Page	k	0.2077	0.3979	0.0181	1.7105
	n	0.8463	0.7372	0.0425	0.8876
Modified page	k	0.3935	0.5250	0.6783	1.3555
	n	0.3935	0.5250	0.6783	1.3555
Henderson and Pabis	a	0.9392	0.9398	0.0231	0.9604
	k	1.6631	0.1424	0.0141	1.7332
Logarithmic	a	0.9316	0.9316	1.0284	0.9588
	k	0.1480	0.1480	0.4255	1.7425
	c	0.0128	0.0128	0.0329	0.0021
Two-term	a	0.4802	0.8960	0.5000	0.5020
	k_0	1.7332	0.1342	1.8375	0.4622
	b	0.4802	0.1049	0.5000	0.5020
	k_1	1.7332	2.5182	1.8375	0.4622
Two-term exponential	a	0.9981	0.9981	1.5488	0.9987
	k	0.1396	0.1396	0.5657	1.0000
Wang and Singh	a	-0.8803	-0.1419	-0.1419	-0.8803
	b	0.1658	0.0047	0.0047	0.1658
Diffusion approximation	a	3.5975	1.0000	1.0023	1.1002
	k	0.1548	0.2756	0.4601	1.8375
	b	0.6981	1.0034	1.0004	1.0013
Midilli-Kucuk	a	0.9967	1.0029	0.9790	0.9783
	k	2.0843	0.4080	0.4063	1.6924
	n	1.6277	0.6978	1.0974	0.9215
	b	-0.2393	-0.0013	-0.0015	-0.0007

Despite the fact that the correlation coefficient "r^2" maintains a consistently high level across the ten empirical models, spanning a range from 0.8241 to 0.9954, it is notable that the Page model exhibited the highest mean "r^2" value of 0.9954, along with the lowest values for the reduced chi-square ($\chi^2 = 0.0070$) and root mean square error ($RMSE = 0.0006$). This model was observed to provide a robust description of the drying characteristics of

Table 7 The estimated kinetic parameters of the fitted mathematical models describing the kinetics of black soldier fly larvae

Models	r^2	χ^2	*RMSE*
Newton	0.9878	0.0218	0.0014
Page	0.9954	0.0070	0.0006
Modified page	0.9869	0.0218	0.0015
Henderson and Pabis	0.9929	0.0289	0.0008
Logarithmic	0.9945	0.0083	0.0007
Two-term	0.9946	0.0062	0.0006
Two-term exponential	0.9491	0.0694	0.0066
Wang and Singh	0.8241	0.2635	0.0223
Diffusion approximation	0.9859	0.0218	0.0016
Midilli-Kucuk	0.9763	0.1305	0.0335

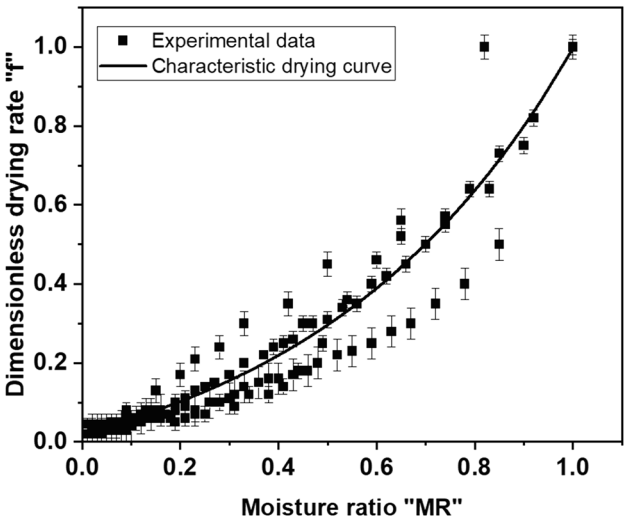

Fig. 9 Characteristic drying curve of black soldier fly larvae

BSFL within the temperature range from 40 °C to 70 °C. Figure 7 demonstrates a strong concurrence between the experimental moisture content and the predicted values obtained through the application of the Page model, for all drying temperatures.

Determination of the Characteristic Drying Curve

Figure 9 presents the characteristic drying curve, which serves as a summary of the results derived from drying BSFL experiments. The approach employed involves normalizing the drying kinetics of BSFL into a theoretical model-based experience. This process includes formulating an exponential equation for moisture ratio (MR) through the application of nonlinear optimization, utilizing the Levenberg–Marquardt algorithm. The dimensionless drying rate (f) can be calculated by aligning the experimental data with the characteristic drying curves of BSFL as outlined below:

$$f = 0.142 * exp(2.05 * MR) - 0.118 \quad (39)$$

To assess the goodness of fit, three criteria were used: the coefficient of determination ($r^2 = 0.984$), the root mean square error ($RMSE = 0.012$) and the reduced ki-square test ($\chi^2 = 0.003$). The distinctive advantage of this characteristic curve lies in its ease of use and unique nature since it considers the mutual interactions between the thermal properties of the drying air and the behavior of BSFL as they undergo the drying process.

Effective Moisture Diffusivity and Activation Energy

Table 8 shows the effective moisture diffusivity values (D_{eff}) at various drying temperatures, while Fig. 10 illustrates the graphs of the diffusive model fitted to the experimental data. Observing that a rise in the drying temperature by 10 °C, from 40 to 70 °C, resulted in a progressive enhancement of the diffusional process by 29.11%, 34.76%, and 145.79%, respectively. However, D_{eff} experienced a substantial increase of 327.00% when the drying temperature was raised by 30 °C (from 40 to 70 °C). A notable enhancement in the diffusional process is achieved with an increase in the drying temperature, reinforcing the experimental results obtained for the drying kinetics. Increasing the drying temperature led to a rise in the partial pressure within the larvae, which exceeded the surface pressure. This facilitated water movement and enhanced the drying rate, as documented in references [74, 75]. The diffusive model, fitted to the experimental data, demonstrates a strong fit with high r^2 values and low χ^2, as shown in Fig. 10. This validates the use of the diffusive model for determining the D_{eff} values.

The D_{eff} values fall within the range estimated in the literature for insects, such as yellow mealworm larvae (4.85×10^{-11} to 1.62×10^{-10} m^2/s) [16] and BSFL dried using a forced-air oven (0.7002×10^{-10} m^2/s to 2.792×10^{-10} m^2/s) [76]. Nevertheless, these values are lower than the ones observed in house crickets (4.78×10^{-9} to 1.31×10^{-8} m^2/s) [72]. This distinction can be ascribed to the influence of moisture diffusivity on the product, which is contingent upon its composition, structure, and insect species [77]. For dried food products, the values of D_{eff} reported from recent investigations typically vary between 10^{-8} and 10^{-12} m^2/s [78].

The activation energy was determined through the graphing of ln D_{eff} against the reciprocal of the temperature ($1/T_{abs}$). This graph exhibited a linear relationship, with the slope representing ($-E_a/R$). The calculated activation energy was 48.66 kJ/mol, falling within the typical range of 12.7–110 kJ/mol observed in various food materials [79] and aligns with the range observed for insects, falling between 30.74 and 52.1 kJ/mol [16, 72, 76]. The variations in E_a values can be ascribed to disparities in cellular structure and chemical composition [77].

Table 8 Effective moisture diffusivity and activation energy values of dried black soldier fly larvae

Temperature (°C)	D_{eff} (m^2/s)	r^2	χ^2	E_a (kJ/kg)	r^2
40	6.15×10^{-11}	0.9989	1.77×10^{-2}	48.66	0.9991
50	7.94×10^{-11}	0.9977	2.63×10^{-2}		
60	1.07×10^{-10}	0.9997	1.55×10^{-3}		
70	2.63×10^{-10}	0.9991	6.92×10^{-3}		

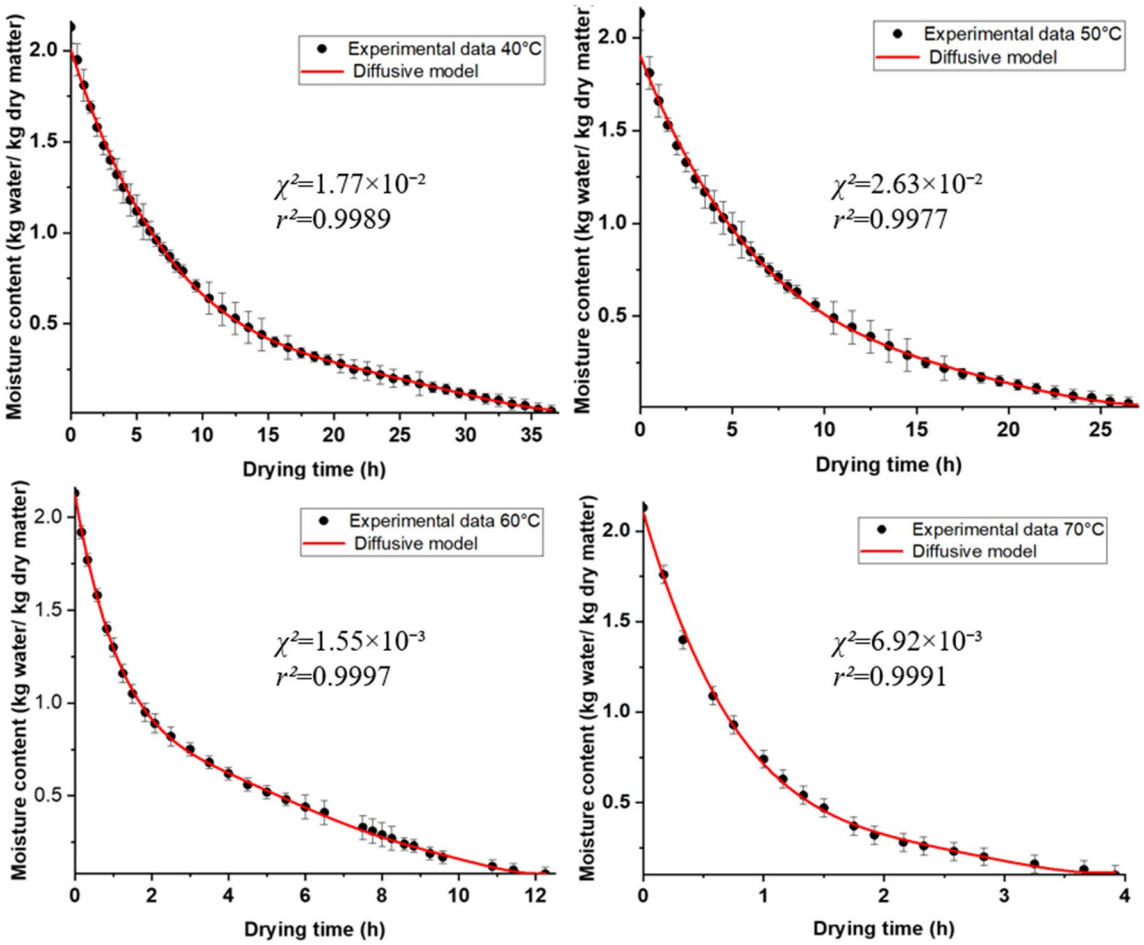

Fig. 10 Diffusive model fitted to the experimental data

Characterization of Black Soldier Fly Larvae

The proximate composition of dried BSFL at four temperatures: 40, 50, 60 and 70 °C using a forced-air oven is given in Table 9.

The drying technique had a statistically significant impact ($P < 0.05$) on the nutritional composition of BSFL, as detailed in Table 9. Drying led to a notable reduction in the moisture content of BSFL. Raw thawed larvae exhibited the initial highest moisture content (2.13 kg water/kg dry

Table 9 Proximate composition of dried BSFL at four temperatures (g/100 g dry matter, n = 3; mean ± standard error)[a]

Parameters[b]	Raw	Dried at 40 °C	Dried at 50 °C	Dried at 60 °C	Dried at 70 °C
Water content (dry basis)	$2.13^{a} \pm 0.76$	$0.10^{b} \pm 0.52$	$0.10^{b} \pm 0.17$	$0.09^{b} \pm 0.12$	$0.08^{b} \pm 1.26$
Protein (g/100 g)	$47.37^{a} \pm 0.07$	$45.29^{b} \pm 0.07$	$43.80^{bc} \pm 0.35$	$41.63^{d} \pm 0.36$	$39.67^{e} \pm 0.47$
Lipid (g/100 g)	$35.87^{a} \pm 0.52$	$33.84^{b} \pm 0.49$	$27.90^{c} \pm 0.34$	$23.34^{d} \pm 0.37$	$23.24^{e} \pm 0.33$
Ash (g/100 g)	$7.5^{b} \pm 0.13$	$8.78^{a} \pm 0.01$	$8.33^{a} \pm 0.06$	$7.79^{a} \pm 0.62$	$7.68^{a} \pm 0.02$
pH	$5.74^{d} \pm 0.01$	$5.99^{c} \pm 0.01$	$7.14^{b} \pm 0.02$	$7.25^{b} \pm 0.01$	$7.64^{a} \pm 0.02$
L^*	$43.73^{a} \pm 0.20$	$35.58^{c} \pm 0.07$	$36.93^{b} \pm 0.31$	$33.38^{d} \pm 0.25$	$31.52^{e} \pm 0.05$
a^*	$4.14^{b} \pm 0.14$	$5.02^{a} \pm 0.05$	$5.74^{a} \pm 0.05$	$5.10^{a} \pm 0.03$	$4.45^{a} \pm 0.01$
b^*	$19.18^{a} \pm 0.07$	$14.37^{a} \pm 0.02$	$16.89^{a} \pm 0.08$	$19.01^{a} \pm 0.25$	$19.91^{a} \pm 0.2$
ΔE	Reference	$9.51^{c} \pm 0.11$	$7.35^{d} \pm 1.45$	$10.39^{b} \pm 0.78$	$12.23^{a} \pm 0.23$

[a]Different superscripts for the same row indicate significant difference ($P < 0.05$)

[b]Water content, protein, lipid and ash content are expressed as a percentage (%) of the dry matter

matter), whereas dried larvae had a moisture content of less than 0.10 kg water/kg dry matter, indicating that drying represents an effective method for preserving and prolonging BSFL's shelf life while simultaneously mitigating its vulnerability to degradation resulting from humidity. Moreover, such low moisture contents imply that the dried BSFL can be stored at ambient temperature [80].

Crude protein content of BSFL (45.29–39.67%) fell within the ranges (45.70–36.5%) reported in previous studies [18, 81]. This protein content is highly competitive in the market, not only meeting but also surpassing the minimum requirement of 34% set by leading companies in the insect production industry [82, 83]. The fat content in our study (ranging from 35.87% to 23.24%) matched the fat levels (ranging from 38.36% to 21.24%) [18, 81, 84]. The variability in protein and fat content depends on various factors, encompassing the age of the larvae at the time of harvest, the rearing substrate employed, and the treatment method applied [85, 86]. Drying had a significant impact on the crude protein and crude fat content of BSFL, with a decrease observed after drying when compared to fresh larvae. As the drying temperature rises, the rate of protein and lipid loss also increases. This can be related, on the one hand, to protein denaturation and/or browning reactions that utilize some of the amino acids, resulting in a decrease in protein content, and on the other hand, to accelerated fat oxidation due to increasing drying temperature, leading to a decrease in lipid content [87, 88].

Ash content of the dried BSFL differed significantly ($P < 0.05$) from that of raw thawed larvae. A significant increase ($P < 0.05$) in the ash content was observed following drying, which can be attributed to an increase in mineral levels [89].

The pH was influenced by the drying process, where an observed correlation indicates that higher levels of heat treatment result in an elevation of pH. This phenomenon may be attributed, firstly, to the degradation of lipases during drying, thereby reducing the acidity of fats [90]. Secondly, it may also be ascribed to the breakdown of heat-sensitive acids, potentially leading to an increase in pH [91].

The process of drying has the potential to alter the perception of a product's color due to variations in refractive indices between water and air, along with structural shrinkage of the product [92, 93]. As a dried product contains reduced water content, it may exhibit reduced light reflection, leading to diminished lightness, as observed in our study when comparing dried larvae to fresh larvae. Drying the larvae led to a noticeable increase in the darkening effect. As expected, this darkening effect was less pronounced when drying at lower temperatures, such as 40 °C and 50 °C, as indicated by the L^* values, in contrast to drying at higher temperatures, like 70 °C. Hence, the rise in drying temperature resulted in a decrease in L^* values, indicating that drying darkened the larvae. Dried larvae exhibit higher a^* values in comparison to fresh larvae, a phenomenon likely attributed to the breakdown of the anthocyanin compounds during Maillard reactions, leading to a change in the natural color of the larvae [94]. As a result, the dried larvae appear to have a more pronounced shift in their coloration. The difference in color between dried larvae and fresh larvae is noticeable and perceptible ($\Delta E \geq 2$), making it readily identifiable to the naked eye [90]. Such color difference can be attributed to the thermal degradation and formation of brown pigments following melanosis at higher temperatures [16]. This darkening effect can be promoted by the enzymatic browning reaction or the oxidation of polyphenols in an aerobic environment or also following the Maillard reaction (non-enzymatic browning reaction) [95]. The best color preservation was obtained at lower temperatures, especially drying at 50 °C.

Conclusion

A comprehensive analysis of the adsorption–desorption isotherms, drying kinetics, and nutritional quality of BSFL was conducted at 40 °C, 50 °C, 60 °C, and 70 °C using a forced-air oven. The key findings are as follows:

- The isotherms were identified as type II, with the hysteresis phenomenon observed. Temperature impacted BSFL's moisture sorption, with equilibrium water content decreasing as temperature increased.
- Peleg's model was found to be the most suitable for describing the sorption isotherm of BSFL within the studied temperature range.
- The optimal water activity for the conservation and storage of BSFL was determined to be 0.38.
- The compensation theory was validated, confirming that the adsorption process is a non-spontaneous reaction driven by enthalpy.
- The Page model provided the best representation of BSFL's drying kinetic.
- Effective moisture diffusivity values increased with temperature, ranging from 6.15×10^{-11} to 2.63×10^{-10} m^2/s, with an activation energy of 48.66 kJ/mol.
- The dried larvae had a protein content of 45.29% to 39.67%, surpassing the 34% minimum requirement set by leading insect production companies, making them highly competitive.
- Higher drying temperatures negatively impact the quality of the larvae.

These findings offer valuable insights for improving drying processes, formulating high-quality finished products, and developing new applications for dried BSFL in areas such as animal feed and human food. This study provides a

solid foundation for future research aimed at maximizing the efficient and sustainable use of dried BSFL.

Author Contributions **Manal Lehmad:** conceptualization, methodology, resources, writing original draft, writing-review and editing. **Youssef El Hachimi:** conceptualization, methodology, writing-review and editing. **Patrick Lhomme:** resources, writing-review and editing. **Safa Mghazli:** methodology, writing-review and editing. **Naji Abdenouri:** project administration, conceptualization, methodology, writing-review and editing.

Funding The research institute for solar energy and new energies (IRESEN) supported this work as part of the project SSH. This work was conducted with the support of the national center of scientific and technical research of Morocco (CNRST), through the research excellence grant program [grant number: 21 UCA2022].

Data Availability No datasets were generated or analysed during the current study.

Declarations

Conflict of interest The authors declare no competing interests.

References

1. L.A. Cadinu, P. Barra, F. Torre, F. Delogu, F.A. Madau, Sustainability **12**, 4567 (2020)
2. G. Sogari, S. BellezzaOddon, L. Gasco, A. van Huis, T. Spranghers, S. Mancini, Animal **17**, 100904 (2023)
3. Y. Weinreis, C.M. Baum, S. Smetana, Sustain. Prod. Consum. **35**, 28 (2023)
4. L. Puente-Díaz, R. Lemus-Mondaca, Rev. Chil. Nutr. **51**, 63 (2024)
5. S. Siva Raman, L.C. Stringer, N.C. Bruce, C.S. Chong, J. Clean. Prod. **373**, 133802 (2022)
6. S. Hasnol, K. Kiatkittipong, W. Kiatkittipong, C.Y. Wong, Processes **8**, 523 (2020)
7. E.A. Wikurendra, N. Herdiani, Hum. Care J. **5**, 966 (2020)
8. T. Liu, T. Klammsteiner, A.M. Dregulo, V. Kumar, Y. Zhou, Z. Zhang, M.K. Awasthi, Sci. Total. Environ. **833**, 155122 (2022)
9. K.C. Surendra, J.K. Tomberlin, A. van Huis, J.A. Cammack, L.-H.L. Heckmann, S.K. Khanal, Waste Manag. **117**, 58 (2020)
10. M.V. Santos, N. Ranalli, J. Orjuela-Palacio, N. Zaritzky, J. Food Eng. **364**, 111796 (2024)
11. A. Al-Muhtaseb, W.A. McMinn, T.R. Magee, Food Bioprod. Process. **80**, 118 (2002)
12. Z. Tagnamas, A. Idlimam, A. Lamharrar, J. Clean. Prod. **434**, 139848 (2024)
13. G. Ghoshal, in *Food Processing for Increased Quality and Consumption*, ed. by A.M. Grumezescu, A.M. Holban (Academic Press, London, 2018), pp. 29–65 https://doi.org/10.1016/B978-0-12-811447-6.00002-3
14. S.K. Amit, M.M. Uddin, R. Rahman, S.M.R. Islam, M.S. Khan, Agric. Food Secur. **6**, 1 (2017)
15. R. Osae, M.T. Apaliya, E. Kwaw, R.S. Akoto, E. Bonah, P. Owusu-Ansah, R.N. Alolga, J. Agric. Food Res. **12**, 100584 (2023)
16. D. Azzollini, A. Derossi, C. Severini, J. Insects as Food Feed **2**, 233 (2016)
17. E. Kamau, C. Mutungi, J. Kinyuru, S. Imathiu, C. Tanga, H. Affognon, S. Ekesi, D. Nakimbugwe, K.K.M. Fiaboe, Food Res. Int. **106**, 420 (2018)
18. M. Lehmad, N. Hidra, P. Lhomme, S. Mghazli, Y. EL Hachimi, N. Abdenouri, Renew. Energy **226**, 120401 (2024)
19. C. Monisha, M. Loganathan, J. Food Process. Preserv. **46**, e16184 (2021)
20. C. Huang, W. Feng, J. Xiong, T. Wang, W. Wang, C. Wang, F. Yang, Eur. Food Res. Technol. **245**, 11 (2019)
21. International Platform of Insects for Food and Feed, Guide on good hygiene practices for European Union (EU) producers of insects as food and feed. (IPIFF, 2024), https://ipiff.org/wp-content/uploads/2024/02/Folder-IPIFF_Guide_A4_19.02.2024_black-colour.pdf. Accessed 05 June 2024
22. E.A. Penner, S.J. Schmidt, J. Food Meas. Charact. **7**, 185 (2013)
23. H. Moussaoui, Y. Bahammou, A. Idlimam, A. Lamharrar, N. Abdenouri, Food Bioprod. Process. **114**, 12 (2019)
24. Y. Bahammou, H. Moussaoui, H. Lamsayeh, Z. Tagnamas, M. Kouhila, R. Ouaabou, A. Lamharrar, A. Idlimam, Sol. Energy **201**, 916 (2020)
25. J.A. Enderby, Trans. Faraday Soc. **51**, 106 (1955)
26. M. Peleg, J. Food Process Eng **16**, 21 (1993)
27. C.R. Oswin, J. Chem. Technol. Biotechnol. **65**, 419 (1946)
28. T.L. Thompson, R.M. Peart, G.H. Foster, Trans. ASAE **11**, 582 (1968)
29. S.E. Smith, J. Am. Chem. Soc. **69**, 646 (1947)
30. G. Halsey, J. Chem. Phys. **16**, 931 (1948)
31. C. Van den Berg, S. Bruin, in *Water activity—influences on food quality*, ed. by L.B. Rockland, G.F. Stewart (Academic Press, New York, 1981), pp.1–64
32. R.R. Krug, W.G. Hunter, R.A. Grieger, J. Phys. Chem. **80**, 2335 (1976)
33. R.R. Krug, W.G. Hunter, R.A. Grieger, J. Phys. Chem. **80**, 2341 (1976)
34. W.P. Da Silva, A.F. Rodrigues, C.M.D.P.S.E. Silva, D.S. De Castro, J.P. Gomes, J. Food Eng. **166**, 230 (2015)
35. J.R. O'Callaghan, D.J. Menzies, P.H. Bailey, J. Agric. Eng. Res. **16**, 223 (1971)
36. Y.C. Agrawal, *Thin layer drying studies for short grain rice*, 1st edn. (Michigan, ASAE, 1977), p.3531
37. G.M. White, I.J. Ross, C.G. Poneleit, Trans. ASAE **24**, 466 (1981)
38. G.E. Page, Factors influencing the maximum rates of air drying shelled corn in thin layers. (Purdue University, 1949), https://docs.lib.purdue.edu/dissertations/AAI1300089/. Accessed 12 Feb 2024
39. A. Yağcıoğlu, A. Değirmencioğlu, F. Çağatay, Drying characteristics of laurel leaves under different drying conditions, in 7th International Congress on Agricultural Mechanization and Energy, Adana, Turkey (1999), pp. 565–569
40. S.M. Henderson, Trans. ASAE **17**, 1167 (1974)
41. Y.I. Sharaf-Eldeen, J.L. Blaisdell, M.Y. Hamdy, Trans. ASAE **23**, 1261 (1980)
42. C. Moyne, N. Kechaou, P.J.D.A. Sobra, I.M. Roques, A. Cairault, H. Bizot, Entropie Thermodyn. – Énergie – Environ. – Économie **167**, 9 (1992)
43. A.S. Kassem, Comparative studies on thin layer drying models for wheat, in 13th International Congress on Agricultural Engineering, Rabat, Morocco (1998), pp. 2–6.
44. A. Midilli, H. Kucuk, Z. Yapar, Dry. Technol. **20**, 1503 (2002)
45. D.A. van Meel, Chem. Eng. Sci. **9**, 36 (1958)
46. P.L. Ferreira, W.P. Silva, A.J.M. Queiroz, R.M.F. Figueir, J.P. Gomes, B.A. Melo, D.C. Santos, T.L.B. Lima, R.R.C. Branco, I. Hamawand, A.G.B. Lima, Foods **9**, 1818 (2020)
47. W.P. da Silva, J.W. Precker, C.M.D.P.S. Silva, J.P. Gomes, J. Food Eng. **98**, 302 (2010)

48. A.V. Luikov, *Analytical Heat Conduction Theory*, 1st edn. (Academic Press, New York, 1968), p.702
49. J. Crank, *Mathematics of Diffusion*, 2nd edn. (Oxford University Press, London, 1975), p.414
50. W.P. Silva, J.W. Precker, C.M.D.P.S. Silva, D.D.P.S. Silva, J. Food Eng. **95**, 298 (2009)
51. W.P. Silva, C.M.D.P.S. Silva, Convective Adsorption-Desorption. (LAB Fit, 2008), https://www.labfit.net/Convective.htm. Accessed 12 July 2024
52. W.P. Silva, V.S. Farias, G.A. Neves, A.G. Lima, Heat Mass Transf. **48**, 809 (2012)
53. R.H. Janssen, J.P. Vincken, L.A.M. Van Den Broek, V. Fogliano, C.M.M. Lakemond, J. Agric. Food Chem. **65**, 2275 (2017)
54. A. ZungurBastıoğlu, M. Koç, F. KaymakErtekin, J. Food Meas. Charact. **11**, 1295 (2017)
55. I. Majid, S. Hussain, V. Nanda, J. Food Meas. Charact. **13**, 775 (2019)
56. S.-H. Ko, G.-P. Hong, S.-G. Min, M.-J. Choi, Dry. Technol. **26**, 1396 (2008)
57. L. Hssaini, R. Ouaabou, J. Charafi, A. Idlimam, A. Lamharrar, R. Razouk, H. Hanine, South African J. Bot. **145**, 265 (2022)
58. S. Motri, T. Amira, in *Advances in the Modelling of Thermodynamic Systems*, ed by E. Essefi, I. Jendoubi (IGI Global, Pennsylvania, 2022), pp. 63–79
59. S. Brunauer, L.S. Deming, W.E. Deming, E. Teller, J. Am. Chem. Soc. **62**, 1723 (1940)
60. K.S. Sing, R.T. Williams, Adsorpt. Sci. Technol. **23**, 839 (2005)
61. F.J. Trujillo, P.C. Yeow, Q.T. Pham, J. Food Eng. **60**, 357 (2003)
62. M.G. Martins, D.E.G. Martins, R.D.S. Pena, LWT - Food Sci. Technol. **62**, 144 (2015)
63. S. Mghazli, A. Idlimam, M. Mahrouz, L. Lahnine, N. Hidar, M. Ouhammou, M. Mouhib, S. Zantar, M. Bouchdoug, Ind. Crops Prod. **88**, 28 (2016)
64. M. Caurie, Int. J. Food Sci. Technol. **42**, 45 (2007)
65. G. V. Barbosa-Cánovas, J. A. J. Fontana, S. J. Schmidt, T. P. Labuza, *Water Activity in Foods: Fundamentals and Applications*, 2nd edn. (John Wiley & Sons, 2020), pp. 3–28
66. S. Cenkowski, D.S. Jayas, D. Hao, Can. Agric. Eng. **34**, 281 (1992)
67. A. Nascimento, M.E.R.M.C. Maria, E.M. Duarte, M. Pasquali, H.M. Lisboa, J. Food Process Eng **42**, e13228 (2019)
68. A. Benseddik, H. Bensaha, D. Lalmi, A. Benahmed-djilali, A. Azzid, J. Renew, Energies Rev. Des Energies Renouvelables **24**, 75 (2021)
69. U. Ryde, Medchemcomm **5**, 1324 (2014)
70. H.W. Park, W.B. Yoon, Dry. Technol. **37**, 1228 (2019)
71. S. Mghazli, M. Ouhammou, N. Hidar, L. Lahnine, A. Idlimam, M. Mahrouz, Renew. Energy **108**, 303 (2017)
72. B. Tanwanichkul, Eng. Access **9**, 56 (2023)
73. L. Bi, B. Liu, Z. Yang, T. Zou, S. Zhao, P. E. Theodorakis, Dry. Technol. **41,** 1397 (2022)
74. R.C. de Sousa, A.B.S. Costa, M.D.M. Freitas, M.T.B. Perazzini, H. Perazzini, Food Bioprod. Process. **143**, 102 (2024)
75. T. Hadibi, D. Mennouche, A. Boubekri, S. Chouicha, M. Arici, W. Yunfeng, L. Ming, F. Fang-ling, Renew. Energy **218**, 119291 (2023)
76. M.N.C. Pinheiro, N. Ribeiro, P. da Silva, R. Costa, J. Insects as Food Feed **8**, 469 (2022)
77. N. Hidar, M. Ouhammou, S. Mghazli, A. Idlimam, A. Hajjaj, M. Bouchdoug, A. Jaouad, M. Mahrouz, Renew. Energy **161**, 1176 (2020)
78. T. Hadibi, A. Boubekri, D. Mennouche, A. Benhamza, N. Abdenouri, Renew. Energy **170**, 1052 (2021)
79. N.P. Zogzas, Z.B. Maroulis, D. Marinos-Kouris, Dry. Technol. **14**, 2225 (1996)
80. D. Vandeweyer, S. Lenaerts, A. Callens, L. Van Campenhout, Food Control **71**, 311 (2017)
81 L. Saucier, C. Mballou, C. Ratti, M.-H. Deschamps, Y. Lebeuf, G.W. Vandenberg, J. Insects as Food Feed **8**, 45 (2021)
82. D.I. Enviroflight, Enviroproducts: Black soldier fly larvae ingredients. (2023), https://d1ip4j1950xau.cloudfront.net/user_upload/EnviroProducts%20Basic%20Specs_JUL2023.pdf. Accessed 26 Feb 2024
83. K.Plume, Insect farms gear up to feed soaring global protein demand. (Reuters, 2018), https://www.reuters.com/article/world/insect-farms-gear-up-to-feed-soaring-global-protein-demand-idUSKBN1HK2AH/. Accessed 18 Mar 2024
84. N.F.N.M. Zulkifli, A.Y. Seok-kian, L.L. Seng, S. Mustafa, Y.-S. Kim, R. Shapawi, PLoS ONE **17**, e0263924 (2022)
85. A. Caligiani, A. Marseglia, A. Sorci, V. Lolli, L. Maistrello, S. Sforza, Food Res. Int. **116**,812 (2018)
86. M. Yusuf, M. Putra, M. Arifuddin, J. Asia. Pac. Entomol. **25**, 101902 (2022)
87. P.T. Akonor, H. Ofori, N.T. Dziedzoave, N.K. Kortei, Int. J. Food Sci. **2016**, 7879097 (2016)
88. G. Melgar-Lalanne, A.J. Hernández-Álvarez, A. Salinas-Castro, Compr. Rev. Food Sci. Food Saf. **18**, 1166 (2019)
89. M. Dandadzi, R. Musundire, A. Muriithi, R.T. Ngadze, Heliyon **9**, e18642 (2023)
90. J. Larouche, M.-H. Deschamps, L. Saucier, Y. Lebeuf, A. Doyen, G.W. Vandenberg, Animals **9**, 182 (2019)
91. A.O. Adetoro, U.L. Opara, O.A. Fawole, Processes **9**, 25 (2021)
92. P.P. Lewicki, J. Food Eng. **61**, 483 (2004)
93. S. Hosseinpour, S. Rafiee, S.S. Mohtasebi, M. Aghbashlo, J. Food Eng. **115**, 99 (2013)
94. S. El Broudi, N. Zehhar, N. Abdenouri, A. Boussaid, A. Hafidi, H. Bouamama, F. Benkhalti, Rev. Mex. Ing. Química **11**, 23 (2022)
95. Y. Zhen, P. Chundang, Y. Zhang, M. Wang, W. Vongsangnak, C. Pruksakorn, A. Kovitvadhi, Appl. Sci. **10**, 6099 (2020)